Ceramics-Silikáty 67 (1), 37-46 (2023)
www.ceramics-silikaty.cz doi: 10.13168/cs.2022.0058

EFFECT OF SULFATE ON THE CHLORIDE DIFFUSION BEHAVIOR OF CORAL AGGREGATE CONCRETE IN THE MARINE TIDE ZONE

#DAGUAN HUANG*, DITAO NIU**, LI SU***, GANG PENG**, QIAN XIA*, YUNHE LIU*

*School of Civil Engineering and Architecture, Xi'an University of Technology, Xi'an 710048, China
**College of Civil Engineering, Xi'an University of Architecture & Technology, Xi'an 710055, China
***School of Civil Engineering, Lanzhou University of Technology, Lanzhou 730050, China

#E-mail: hdg0505@163.com

Submitted November 7, 2022; accepted December 12, 2022

Keywords: Coral aggregate concrete, Chloride, Sulfate, Combined action, Erosion mechanism

This paper studied the effect of sulfate on chloride diffusion behavior in coral aggregate concrete (CAC) in marine tide zone. Three water/binder ratios of CAC were designed for experimental analysis, and the mechanism of the effect of sulfate on chloride transport was investigated by different microscopic experimental methods. The test results show that the chloride content decreases with the decrease of water/binder ratio of CAC. At an equal number of drying-wetting cycles, the chloride content under the combined action of chloride and sulphate is lower than that under the sole action of chloride. The change of peak chloride content with time showed a linear function with the square root of erosion time, while the chloride diffusion coefficient gradually decreased with erosion time. Adding silica fume to CAC effectively reduced the chloride diffusion coefficient, with a decrease of 26.1 % ~ 46.2 %. The attenuation coefficient of CAC under chloride erosion was 16.4 % ~ 38.1 % higher than that under the combined action of chloride and sulfate. The chloride diffusion model was established, and the error between the calculated value of the model and the experimental value was within 16 %. Microscopic observations revealed that in the early stage of erosion, the sulfate erosion products ettringite and gypsum had a compacting effect on the CAC, but in the late stage of erosion, they produced expansion cracks, which accelerated the deterioration of CAC.

INTRODUCTION

Concrete is an important basic material for social development, and it is also the most widely used and produced man-made material with a low price [1]. In recent years, China's marine economy has achieved rapid development and become a new economic growth point. Concrete shows excellent erosion resistance in harsh environments, and is increasingly used in harbors, wave barriers and other marine buildings [2]. However, the South China Sea islands are far from the mainland, and the lack of concrete raw materials on the island will greatly increase the construction cost if the concrete raw materials are transported by conventional sea transportation [3, 4]. Relevant research shows that the main structure of the South China Sea Islands and Reefs is coral reefs. Coral aggregate concrete (CAC) can be prepared by using the coral reefs mined from dredging ports to prepare coral aggregate. Scholars at home and abroad have shown that CAC prepared from coral aggregate can meet the strength requirements of construction, which is of great significance to the construction of island reefs [5, 6].

The durability of concrete has been an inevitable key issue from the beginning of concrete materials applied to marine engineering. Island buildings are di-rectly exposed to the marine environment, and a large amount of Cl^- and SO_4^{2-} in seawater causes the durability problem of island concrete structures to be far more serious than that of land engineering structures [7, 8]. Chloride ions are less aggressive to the concrete material itself, but chloride ions are the most important factor causing reinforcement corrosion. Due to the presence of micro-cracks and pore structures within the concrete, with the increase of time in the service environment, chloride ions will gradually penetrate through the concrete protective layer to reach the surface of the reinforcement, which in turn leads to reinforcement corrosion [9, 10]. At present, relevant scholars have studied the chloride ingress performance of CAC. Huang et al. showed that the diffusion rate of chloride in CAC is greater than that in ordinary aggregate concrete, but the addition of appropriate amounts of fly ash or basalt fibers in CAC can effectively improve the chloride erosion resistance of CAC [11]. Dou et al. also showed that the chloride erosion resistance of CAC is lower than that of ordinary aggregate concrete [12].

Sulfate diffusion into the concrete will produce chemical and physical erosion, which in turn will lead to the expansion and spalling of the concrete. Not only it reduces the mechanical properties of the concrete itself, but it also weakens the protection of the concrete to the internal reinforcement, which will accelerate the time of chloride reaching the surface of the reinforcement [13, 14]. Chen et al. studied the diffusion of Cl^- and SO_4^{2-} under the combined erosion of sulfate and chloride, and the results showed that the diffusion of the two in the concrete will restrain each other in a short time [15]. Jin et al. showed that the presence of sulfate reduces the resistance of concrete to chloride erosion [16]. Du et al. showed that the presence of chloride significantly reduces the degree of concrete sulfate corrosion, and as the chloride content increases the degree of concrete sulfate erosion decreases [17]. Relevant studies have shown that in the water level fluctuation zones such as splash zone and tidal zone, concrete was subjected to both drying-wetting cycles and aggressive ions together, which will accelerate the destruction of concrete structure and thus cause early degradation of concrete structural properties [18, 19]. Until now, there have been few reports on the effect of sulfate on chloride transmission in CAC, resulting in a lack of some basis for the durability design of CAC for island construction.

Following the aforementioned studies, little research has been reported on the effect of sulfate on chloride diffusion in CAC, which to a certain extent affects the durability design of CAC structures and hinders the wide application of CAC. In this paper, the drying-wetting cycle was used to simulate the marine tidal zone, and the erosion tests were conducted on CAC with different water/cement ratios under the chloride erosion, combined chloride and sulfate, respectively. The variation patterns of chloride content, peak chloride content and chloride diffusion coefficient of CAC under the two erosion environments were analyzed and compared, and the effect of sulfate on chloride transport was explored. In addition, experimental methods such as XRD, TG and SEM were used to reveal the mechanism of sulfate effect on chloride diffusion. The results of the study can provide a basis for the design of high-durable CAC.

EXPERIMENTAL

Materials

P.O 42.5R Portland cement (PC), fly ash (FA), and silica fume (SF) were used as cementitious materials to prepare CAC. The chemical composition of cementitious materials is shown in Table 1. The water (W) was the local tap water in Xi'an. The superplasticizer was a polycarboxylic acid high-performance superplasticizer (PBS) with a water-reducing rate of 30 %. The coral aggregate for preparing CAC was taken from the South China Sea. The coral aggregate was divided into coral coarse aggregate and coral fine aggregate after crushing by crusher, as shown in Figure 1.

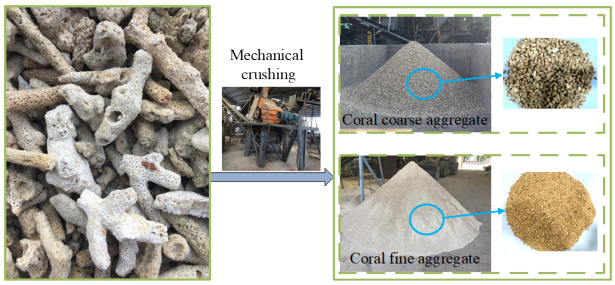

Figure 1. Coral aggregate.

Mix proportions

In this paper, four groups of concrete mixtures were designed as shown in Table 2, where C1, C2 and C3 represent CAC with water/binder ratios of 0.40, 0.35 and 0.25, respectively, and C4 represents CAC with water/binder ratio of 0.35 coral aggregate mixed with 5 % SF.

Table 1. Chemical composition of the cementitious materials (%).

Item	SiO_2	Al_2O_3	Fe_2O_3	CaO	MgO	SO_3	K_2O	Na_2O
OPC	21.18	5.02	3.14	63.42	3.12	2.30	0.65	0.42
FA	35.71	16.57	8.92	21.14	1.41	1.94	0.80	1.02
SF	85.04	0.97	1.04	1.63	0.32	-	0.81	0.19

Table 2. Mix proportions ($kg \cdot m^{-3}$).

Specimen	PC	CA	Sand	Water	FA	SF	W/C
C1	408	736	904	192	72	-	0.40
C2	446.25	600	900	183.75	78.75	-	0.35
C3	595.33	506	768	172.67	107.33	-	0.25
C4	420	600	900	183.75	78.75	26.25	0.35

Test contents

Erosion test

Concrete cube specimens with 100 mm were used in this test, and all specimens were tested after curing at a temperature of 20 ± 2 °C and humidity of 98 % for 28 d. The erosion test was carried out using the drying-wetting cycle method. The erosion solutions were 3.5 % NaCl solution (E1) and 3.5 % NaCl + 5 % Na_2SO_4 solution (E2), respectively, and the solution temperature was 28 °C. Firstly, the specimens were soaked in the erosion solution for 1 day, and then the specimens were taken out of the solution and dried in a blast drying oven at 50 °C for 1 day, and a drying-wetting cycle took 2 days. Five erosion cycles were designed, which were 15, 30, 45, 60 and 90 drying-wetting cycles, respectively. The schematic diagram of the drying-wetting cycle is shown in Figure 2.

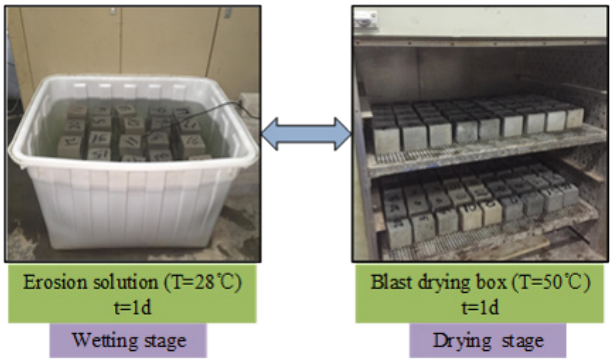

Figure 2. Drying-wetting cycle test.

Chlorine content testing

After reaching the erosion cycle, the free chloride test process was was conducted reference [12]. The free chloride content in concrete was calculated according to Equation 1.

$$W_{[Cl^-]}\% = \left(\frac{M_{[Cl^-]} \times 10^{-P[Cl^-]} \times V}{G} \right) \times 100\% \quad (1)$$

Where: $W_{[Cl\text{-}J]}$ is the free chloride content of CAC (%); $M_{[Cl\text{-}J]}$ is the molar mass of chloride ion, 35.45 g·mol^{-1}. G is the mass of concrete powder used for soaking (g); V is the volume of immersion solution (ml).

Micro test analysis

The physical phase changes of concrete after erosion were tested by X-ray diffraction (XRD) and thermogravimetry (TG), and the microscopic morphological changes of concrete after erosion were observed by scanning electron microscope (SEM).

RESULTS AND DISCUSSION

Distribution of the chloride content

Figure 3 shows the comparison distribution of chloride content of CAC under the erosion of chloride salt and composite salt, respectively. It can be seen that in both erosion environments, the chloride content increases and then decreases with increasing erosion depth, and peak chloride content appear inside the concrete. In addition, at the same erosion depth, the chloride content decreases as the water/cement ratio of CAC decreases. The overall trend is that the chloride content under composite salt erosion is lower than that under chloride salt erosion when the number of drying-wetting cycles is the same. This is because when sulfate and chloride enter the concrete with the erosion solution, the sulfate reacts with the cement hydration products to produce expansive products, which block the transport channels and slow down the chloride diffusion rate [20, 21]. Taking C2 concrete as an example, after 45 drying-wetting cycles, the inflexion point of chloride content appears at 10 mm from the concrete surface under composite salt erosion, and only at 12 mm from the concrete surface under chloride salt erosion. The peak chloride content under the composite salt erosion is small, resulting in the reduction of the driving force of diffusion. With the increase in the number of drying-wetting cycles, the

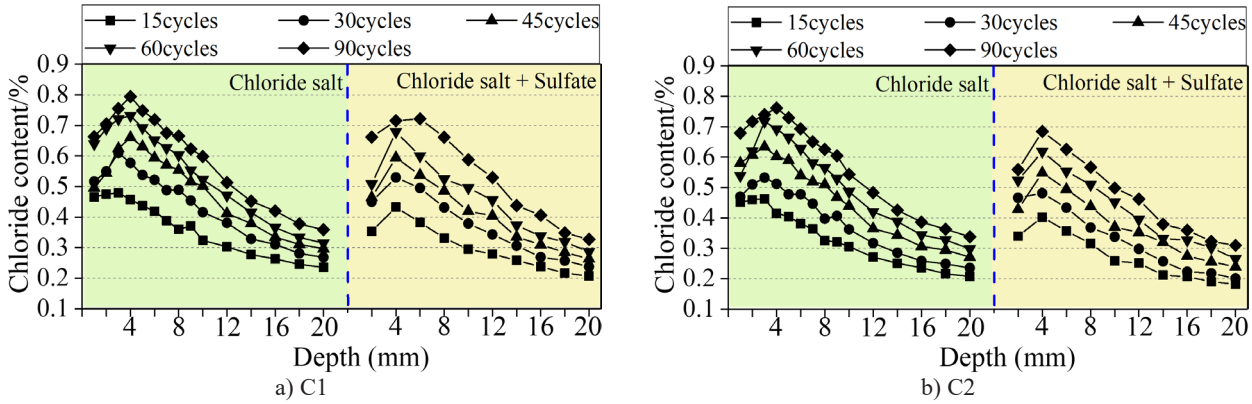

Figure 3. The distribution of the chloride content.

continue on the next page ...

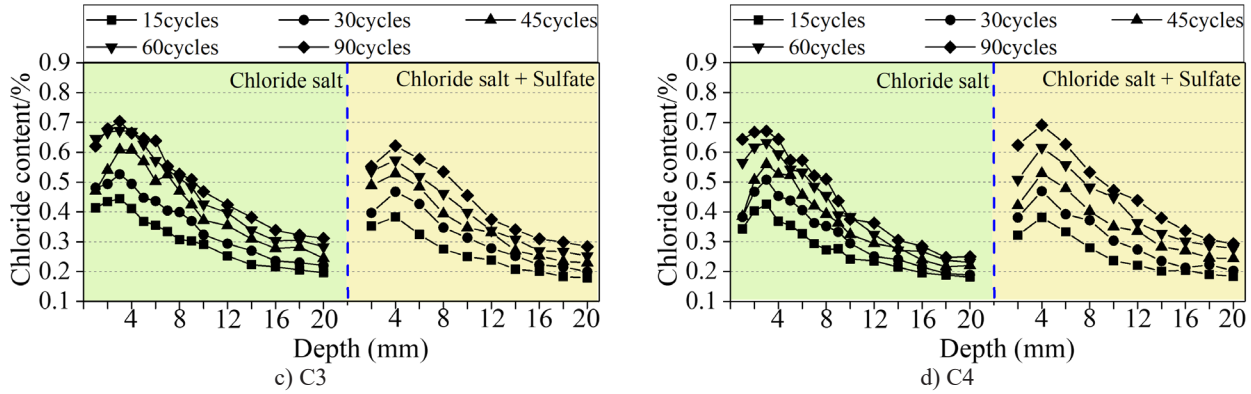

Figure 3. The distribution of the chloride content.

inflexion point of chloride content moves to the interior of concrete. After 60 drying-wetting cycles, the inflexion point of chloride content appears at 14 mm away from the concrete surface under combined salt erosion. In comparison, the inflexion point did not appear until at 16 mm away from the concrete surface under the action of chloride erosion. The content difference between the two erosion environments reached the maximum after 60 drying-wetting cycles. After 90 drying-wetting cycles, the increase of chloride content under composite salt erosion is higher than that under chloride salt erosion.

Peak chloride content

Figure 4 shows the comparison of peak chloride content of CAC under chloride salt and combined salt erosion, respectively. It can be seen that with the increase the number of drying-wetting cycles, the peak chloride content of concrete under combined salt erosion is always low than that under the chloride salt erosion, and the peak chloride content of C2 under combined salt erosion is 9.6 % ~ 13.7 % lower than the value under the chloride salt erosion. In addition, the increase of peak chloride content under chloride salt erosion gradually decreases with the increase in the number of drying-wetting cycles. The peak chloride content of C2 after 30 drying-wetting cycles is 15.2 % higher than that after 15 drying-wetting cycles. In comparison, it is only 6.2 % higher after 90 drying-wetting cycles than that after 60 drying-wetting cycles. Under combined salt erosion,

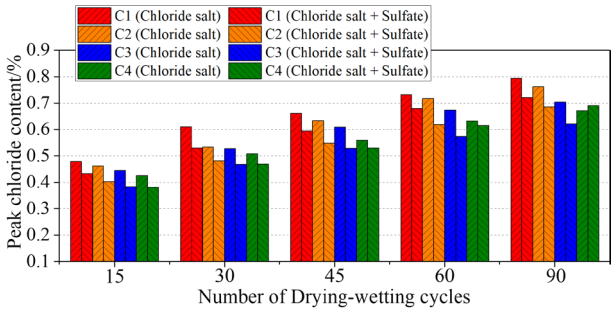

Figure 4. Peak chloride content with the different drying-wetting cycles.

the magnitude of increase in peak chloride content in the late erosion period is higher than that under chloride salt erosion condition, and the peak chloride content was 4.6 % − 8.6 % and 6.3 % − 12.2 % higher after 90 drying-wetting cycles than at 60 drying-wetting cycles under chloride salt and composite salt erosion, respectively.

In the chloride salt erosion environment, with the increase in the number of drying-wetting cycles, the internal hydration reaction of CAC continues, generating more C-S-H gels [22], making the concrete denser and reducing the chloride diffusion rate. Hence, the increase in peak chloride content decreases in the later stages. Under the combined action of chloride and sulfate, sulfate ion will react with $Ca(OH)_2$ and hydrated calcium aluminate in concrete at the initial stage of erosion to produce expansive substances such as gypsum and ettringite. The expansive products fill the internal pores of concrete and block the channel of chloride diffusion [21, 23]. Therefore, the peak chloride content in combined salt erosion environment is less than that in chloride erosion environment. However, with the increase in the number of drying-wetting cycles, the expansive products start to generate expansion stress, which causes microcracks in the concrete, providing new channels for chloride diffusion and accelerating the rate of chloride diffusion into the concrete [24]. Therefore, in the late stage of erosion, the increase of peak chloride content under the combined action of chloride and sulfate is higher than that under the chloride erosion environment.

According to the results of Figure 4, it can be seen that the peak chloride content gradually increases with increasing erosion time. Relevant studies have shown that the change in peak chloride content shows a linear function change with the square root of erosion time, which can be expressed by Equation 2 [25]. The fitting results according to the equation can be obtained as shown in Figure 5. It can be seen that the correlation coefficient R^2 are all greater than 0.95, indicating that the trend of peak chloride content can be well described by using Equation 2.

$$C_p(t) = k\sqrt{t} + b \quad (2)$$

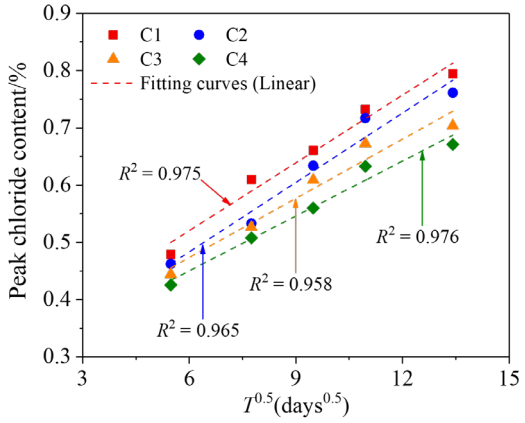

a) Chloride salt

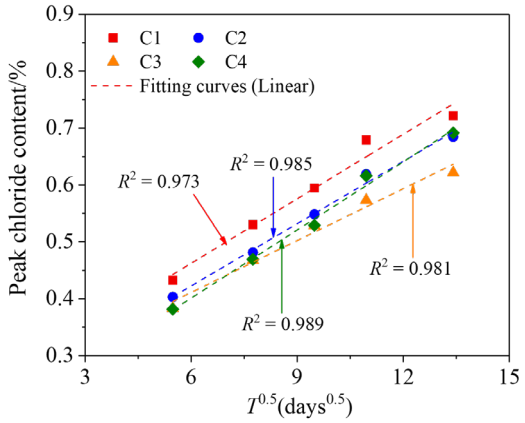

b) Combined of chloride and sulfate

Figure 5. Fitting curves of the time-varying law of the peak chloride concentration.

Chloride diffusion coefficient

The variation pattern of chloride diffusion coefficient of CAC under two erosion environments is shown in Figure 6. It can be seen that the overall trend shows a gradual decrease in the chloride ion diffusion coefficient for all groups of concrete as the number of drying-wetting cycles increases. The smaller the water binder ratio of CAC is, the smaller the chloride ion diffusion coefficient is. Under the condition of chloride salt erosion, the chloride ion diffusion coefficient of C2 concrete is 13.7 % ~ 20.9 % lower than that of C1 concrete, and that of C3 concrete is 28.8% ~ 41.8% lower than that of C1 concrete; under the combined action of chloride salt and sulfate, the chloride ion diffusion coefficient of C2 concrete is 11.2 % ~ 24.5 % lower than that of C1 concrete, and that of C3 concrete is 28.6 % ~ 45.3 % lower than that of C1 concrete. The addition of silica fume to the CAC effectively reduces the chloride ion diffusion coefficient. It can be seen that the chloride ion diffusion coefficient of C4 concrete is 26.1 % ~ 46.2 % lower than that of C2 concrete. At the initial stage of erosion, the chloride ion diffusion coefficients of all groups of concrete under chloride salt erosion were higher than those under compound salt erosion. When the drying-wetting cycles were 60 times, the difference between the chloride ion diffusion coefficients of each group of concrete under the two erosion conditions was small, while when the drying-wetting cycles were 90 times, the chloride ion diffusion coefficients under the composite salt erosion were greater than the values of chloride ion diffusion coefficients under the chloride salt erosion conditions, reaching 6.5 % ~ 25.5 %. Under the coupling action of chloride salt and sulfate, sulfate ion and chloride ion enter the concrete interior through various ways such as capillary adsorption and diffusion. During the process of transport, sulfate ions react with the hydration products of concrete to produce gypsum and ettringite, which block the diffusion channels and thus reduce the ion diffusion rate. However, the increase of erosion products, thus causing concrete surface cracking, leads to increased concrete porosity and microcracks and consequently accelerates the ion diffusion rate. Silica fume refines the pore structure of CAC and slow down the speed of ion diffusion.

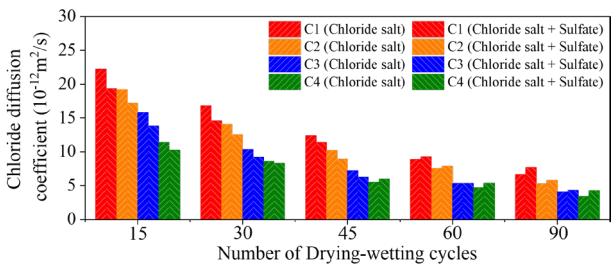

Figure 6. Chloride diffusion coefficient of the concrete specimens.

Attenuation coefficient of the chloride diffusion coefficient

Related studies have shown that the chloride diffusion coefficient presents a power function attenuation trend with increasing exposure time, which can be described by Equation 3 [26].

$$D_a(T) = D_0 \left(\frac{T_0}{T} \right)^m \tag{3}$$

Where, $D_a(T)$ is the chloride diffusion coefficient of concrete at the time of T (10^{-12}m^2·s^{-1}); D_0 is the chloride diffusion coefficient at the reference period T_0 (10^{-12}m^2·s^{-1}); T_0 is the reference value time of diffusion coefficient (d); m is the attenuation coefficient of chloride diffusion coefficient.

The chloride diffusion coefficient of CAC under two erosion environments was fitted by Equation 3. The fitting curves and the attenuation coefficient of chloride diffusion coefficient are shown in Figure 7 and Figure 8, respectively. It can be seen that the fitting correlation coefficient is all greater than 0.9, indicating that the

chloride diffusion coefficient of CAC under the two erosion environments follows to the downward trend of power function, which is the same as the conclusion of Zhang et al [27]. Figure 8 shows that the attenuation coefficients of all groups of CAC under the condition of chloride erosion are more significant than the values under the composite salt erosion. The attenuation coefficient of C1, C2, C3 and C4 under the condition of chloride salt erosion are 27.8 %, 21.7 %, 16.4 % and 38.1 % larger than that under the composite salt erosion, respectively. Therefore, although the chloride diffusion coefficient is relatively small under the combined salts at the early stage of erosion, with the increase of erosion time, the chloride diffusion coefficient decays faster under the condition of chloride erosion, so the chloride under the combined salt erosion may reach the surface of reinforcement earlier, which causes corrosion of reinforcement and adversely affects the durability of the structure.

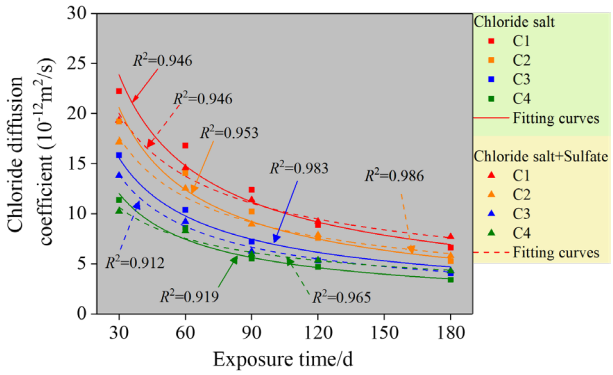

Figure 7. Fitting curves of the chloride diffusion coefficient.

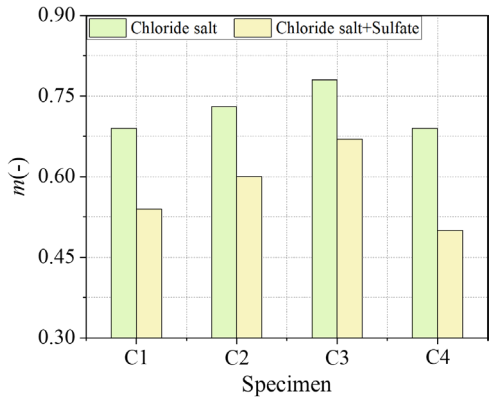

Figure 8. The attenuation coefficient of the CAC.

Chloride diffusion model

There are various diffusion modes of chloride in concrete, and the transmission of chloride is considered to be dominated by diffusion mechanism within the peak chloride content. Therefore, Fick's second law is used to describe the diffusion process of chloride in marine environment in concrete, and the analytical solution can be expressed by Equation 4 [28].

$$C(x,t) = C_s\left[1 - erf\left(\frac{x}{2\sqrt{D_a t}}\right)\right] \quad (4)$$

Where: $C(x, t)$ is the chloride content (%) at the depth x from the concrete surface at erosion time t; C_s is the surface chloride content; x is the depth from concrete surface (mm); D_a is the chloride diffusion coefficient (mm^2·s^{-1}); *erf* is the error function.

The above analysis shows that there is a convection zone inside the concrete under the action of drying-wetting cycles, and the distribution of chloride in this region does not fully comply with Fick's second law. In order to simplify the calculation, the chloride content within the peak chloride content is calculated using Fick's second law. Moreover, the attenuation trend of chloride diffusion coefficient is obtained in the previous section, which can be expressed by power function. The surface chloride content can be replaced by the peak chloride content at this time. Therefore, by substituting Equations 2 and 3 into 4, the chloride content at a given depth and exposure time can be obtained as follows.

This paper verifies the rationality of the chloride

$$C(x,t) = (k\sqrt{t}+b)\left[1 - erf\left(\frac{x}{2\sqrt{D_0\left(T_0/T\right)^m t}}\right)\right] \quad (5)$$

diffusion model with the chloride contents of C2 concrete at different erosion times under the action of chloride salt and composite salt erosion, respectively, and the parameters in the model can be obtained by calculation. The relationship between the calculated results of the chloride diffusion model established in this paper and the experimental data is shown in Figure 9. It can be seen that ignoring the data within 4 mm from the surface concrete, the chloride content calculated by the model is in well agreement with the test results, which proves the rationality of the model established in this paper.

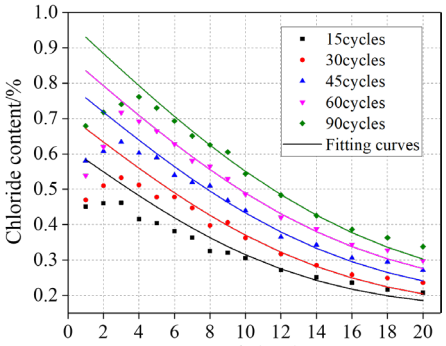

a) Chloride salt

Figure 9. Comparison between the calculated value and experimental value.

continues on the next page ...

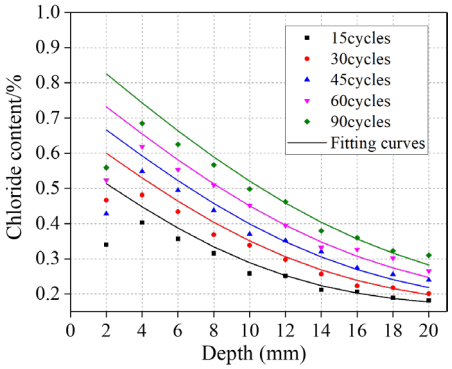

b) Combined of chloride and sulfate

Figure 9. Comparison between the calculated value and experimental value.

Through the chloride diffusion model, the chloride content of C2 after 15, 30, 45, 60 and 90 drying-wetting cycles under the action of chloride salt and composite salt erosion was calculated, respectively. Then comparative analysis was conducted with the experimental values. The results are shown in Figure 10a and 10b, respectively. It can be seen that the error between the predicted value of chloride content and the experimental value of CAC under chloride salt erosion is controlled within 16 %, and the error between the predicted value of chloride content and the experimental value is controlled within 12 % under the composite salt erosion, indicating the high accuracy of the chloride diffusion model.

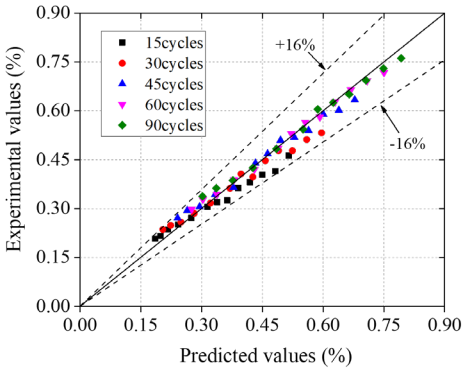

a) Chloride salt

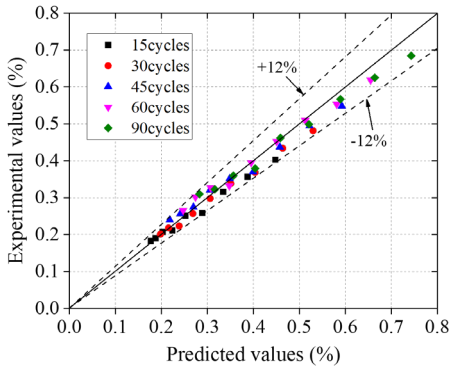

b) Combined of chloride and sulfate

Figure 10. Comparison between the calculated value and experimental value of the chloride content in the C2 concrete.

Microscopic analysis

The XRD patterns and TG results of CAC under the erosion of chloride salt and composite salt are shown in Figure 11 and Figure 12, respectively. It can be seen that the eroded CAC mainly includes aggregate, hydration products and erosion products. The mineral components of aggregate are mainly calcium carbonate and quartz, the hydration products mainly include $Ca(OH)_2$ and calcium silicate, the chloride erosion products are mainly Friedel's salt, and the erosion products under the composite action of chloride and sulfate are mainly ettringite and gypsum. With the increase in drying-wetting cycles, the $Ca(OH)_2$ peak gradually weakened. After 90 drying-wetting cycles, the $Ca(OH)_2$ peak was very weak under the chloride erosion environment, while the $Ca(OH)_2$ peak had disappeared under the composite action of chloride and sulfate. In addition, it can also be seen that the diffraction peaks of gypsum and ettringite in concrete are stronger under the composite action of chloride and sulfate, while no diffraction peaks of gypsum and ettringite appear under the chloride salt environment, indicating that the CAC suffers from sulfate attack, the sulfate ion consumes a large amount of sodium hydroxide and forms gypsum and ettringite. The TG results of CAC is shown in Figure 12, from which it can be seen that the concrete aggregates, hydration products and erosion products have obvious endothermic

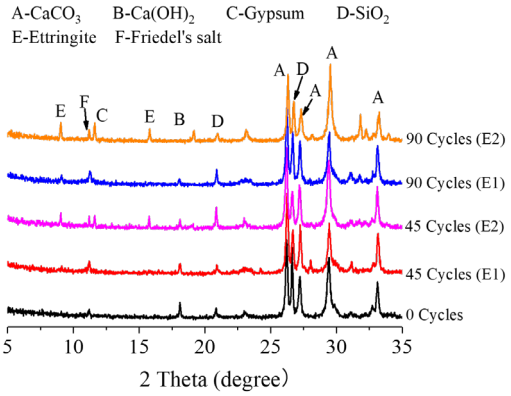

Figure 11. XRD analysis of the CAC.

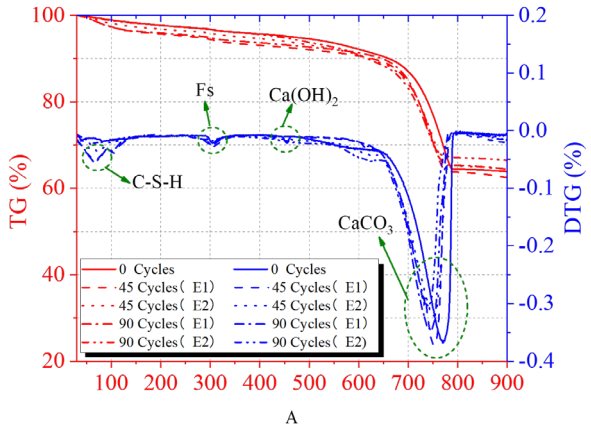

Figure 12. TG/DTG analysis of the CAC.

peaks. The endothermic peak of Friedel's salt is obvious before erosion as well as during erosion, because the coral aggregate itself also has chloride ions [29], so Friedel's salt appears in the concrete before erosion. With the increase in drying-wetting cycles, the endothermic peak of $Ca(OH)_2$ decreases gradually until it disappears. The endothermic peak area of $Ca(OH)_2$ disappears faster under the simultaneous action of chloride and sulfate.

The micro morphology of CAC is observed by SEM, and the influence of different erosion environments on the micro morphology of CAC was analyzed. Figure 13a shows the microscopic morphology of the non-erosion CAC, it can be seen that the internal hydration of the concrete is good, a large amount of hydrated calcium silicate and slab-like calcium hydroxide can be seen, and the concrete structure is relatively dense. Figure 13b shows the micro morphology of CAC under chloride salt environment. It can be seen that after chloride erosion, the porosity of CAC is large, the structure is relatively loose, and some sodium chloride crystals are also found. The hydrated calcium silicate gel inside the concrete shows a flocculent shape, which is due to the continuous decomposition of $Ca(OH)_2$ inside the concrete under the effect of continuous drying-wetting cycle, and the pH value decreases [30]. In addition, the loss of calcium ions in hydrated calcium silicate leads to the decline of the stability and cementation ability of hydrated calcium silicate. Figure 13c shows the internal micro morphology of CAC under the composite action of chloride salt and sulfate. It can be seen that there are obvious needle bar erosion products in the CAC. In addition, short columnar crystals are also found in concrete. The short columnar crystals and needle bar crystals are staggered to form a dense structure. Through energy spectrum analysis, it was found that needle bar and short column erosion

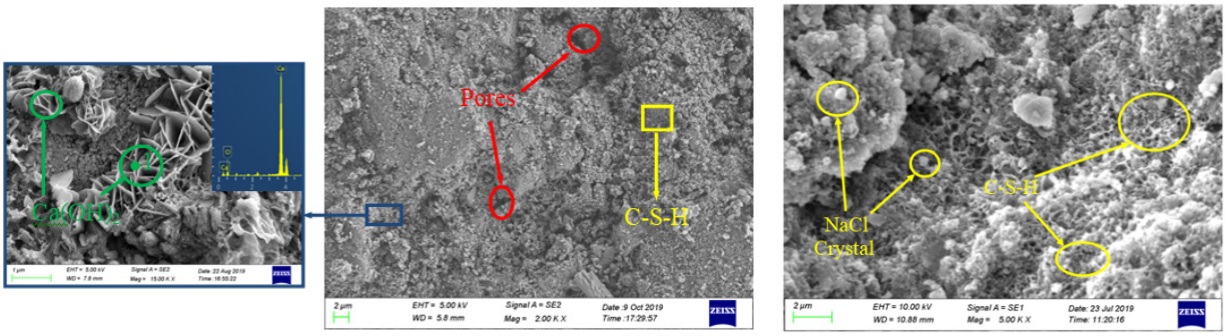

a) Undisturbed environmentt

b) Chloride erosion environment

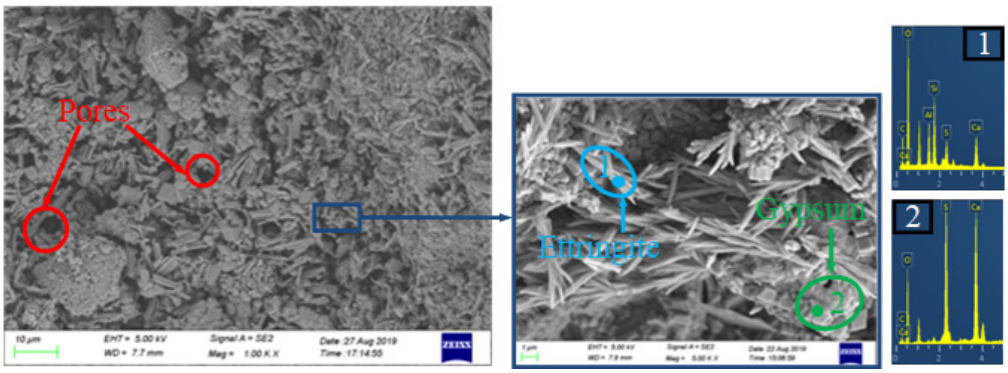

c) Composite chloride and sulfate erosion environment

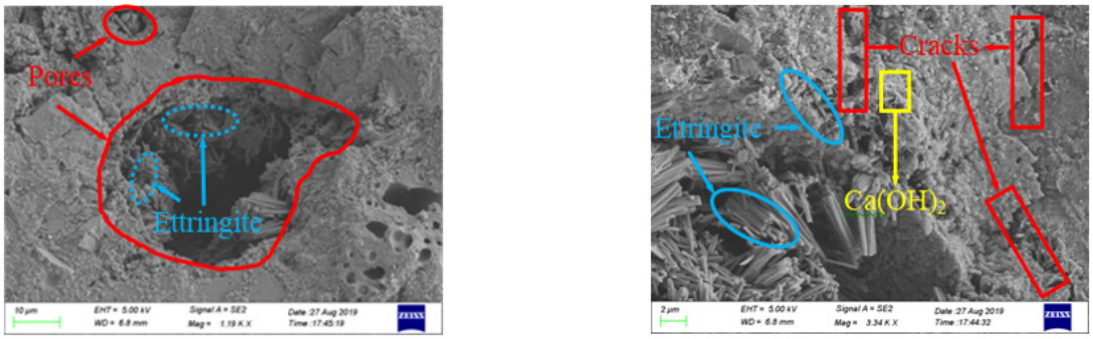

d) Erosion products fill in pores

e) Microcracks appear at the edge of the pores

Figure 13. SEM morphology of the CAC.

products were ettringite and gypsum, respectively. Figure 13d shows the micro morphology of the coral aggregate pores filled with erosion products. It can be seen that erosion products have filled some pores. Initial defects such as microcracks and pores exist inside the CAC. After sulfate ion diffuses into the concrete, it reacts with hydration products to generate ettringite, gypsum and other erosion products, which first fill in the pores and microcracks [31]. Therefore, at the initial stage of erosion, the corrosive products are filled in the pores to strengthen the concrete and make the structure more dense. As the erosion time increasing, expansion cracks will occur when the amount of erosion products reaches a certain amount. As can be seen from Figure13e, after the pores are filled, micro cracks appear at the edge of the pores, which provide more infiltration channels for ion diffusion and accelerate the deterioration of concrete.

CONCLUSIONS

In this paper, the influence of sulfate on chloride diffusion in CAC under drying-weting cycles was studied. The main conclusions were as follows:

1. The chloride content first increases and then decreases with the increase of erosion depth under the erosion of chloride salt and composite salt. Therefore, when the number of drying-wetting cycles is the same, the chloride content under the combined action of chloride and sulfate is smaller than that under the action of chloride.
2. When the number of drying-wetting cycles is the same, the peak chloride content of concrete under the combined action of chloride and sulfate is always smaller than the value under the chloride salt erosion. However, in the late stage of erosion, the increase in peak chloride content under the composite action of chloride and sulfate is larger than the increase in chloride salt erosion. With the increasing number of drying-wetting cycles, the change of peak chloride content with time showed a linear function with the square root of erosion time.
3. The smaller the water-cement ratio of CAC, the smaller the chloride diffusion coefficient. The addition of silica fume to CAC can effectively reduce the chloride diffusion coefficient by 26.1 % ~ 46.2 %. As the number of drying-wetting cycles increased, the chloride diffusion coefficient of all concrete groups showed a gradual decrease. At the initial stage of erosion, the chloride diffusion coefficients under chloride salt erosion were more significant than those under the combined effect of chloride and sulfate. In contrast, the opposite pattern was observed at the end of erosion. The attenuation coefficients of all concrete groups under chloride salt erosion are greater than the values under the composite action of chloride and sulfate.
4. The chloride diffusion model was established, and after comparison and analysis, the error between the calculated value of the model and the experimental value was controlled within 16 %.
5. The chloride erosion products are mainly Friedel's salts, while the erosion products under the composite action of chloride and sulfate are mainly ettringite and gypsum. In the early stage of erosion, the erosion products fill in the pores and play a dense reinforcing effect on the concrete, making the structure more dense. As the continuous increase of erosion time, when the erosion products reach a certain amount, expansion cracks will occur and accelerate the deterioration of concrete.

Acknowledgments

This study is financially supported by National Natural Science Foundation of China (No. 51590914) and Key Project of Scientific Research Program of Shaanxi Provincial Education Department (No. 20JY037).

REFERENCES

1. Qiu D. (2000): Science and technology problems in coastal and offshore engineering. *Journal of Dalian University of Technology, 40* (6), 631-637.
2. Yu H., Da B., Ma H., Zhu H., Yu Q., Ye H., Jing X. (2017): Durability of concrete structures in tropical atoll environment. *Ocean Engineering, 135*, 1-10. doi: 10.1016/j.oceaneng.2017.02.020
3. Liu J., Ju B., Xie W., Yu H., Xiao H., Dong S., Yang W. (2021): Design and Evaluation of an Ultrahigh-Strength Coral Aggregate Concrete for Maritime and Reef Engineering. *Materials, 14*, 5871-5890. doi: 10.3390/ma14195871
4. Huang D., Niu D., Su L., Pan D., Liu Y. (2022): Durability of coral aggregate concrete under coupling action of sulfate, chloride and drying-wetting cycles. *Case Studies in Construction Materials, 16*, e01003. doi: 10.1016/j.cscm.2022.e01003
5. Arumugam R., Ramamurthy K. (1996): Study of compressive strength characteristics of coral aggregate concrete. *Magazine of Concrete Research, 48* (176), 141-148. doi: 10.1680/macr.1996.48.176.141
6. Chen Z., Chen T., Qu J. (1991): A feasibility study of application of coral reef sand concrete. *Ocean Engineering, 9* (3), 67-80.
7. Brown P., Badger S. (2000): The distributions of bound sulfates and chlorides in concrete subjected to mixed NaCl, $MgSO_4$, Na_2SO_4 attack. *Cement and Concrete Research, 30*, 1535–1542. doi: 10.1016/S0008-8846(00)00386-0
8. Santhanam M., Cohen M., Olek J. (2002): Mechanism of sulfate attack: a fresh look: Part 1: Summary of experimental results. *Cement and Concrete Research, 32* (6), 915–921. doi: 10.1016/S0008-8846(02)00724-X
9. Fu Q., Bu M., Zhang Z., Xu W., Yuan Q., Niu D. (2022): Hydration Characteristics and Microstructure of Alkali-

Activated Slag Concrete: A Review. *Engineering*, article in press. doi: 10.1016/j.eng.2021.07.026
10. Shi W., Najimi M., Behrouz S. (2020): Reinforcement corrosion and transport of water and chloride ions in shrinkage-compensating cement concretes. *Cement and Concrete Research, 135*, 106121. doi: 10.1016/j.cemconres.2020.106121
11. Huang D., Niu D., Su L., Liu Y., Guo B., Xia Q., Peng G. (2022): Diffusion behavior of chloride in coral aggregate concrete in marine salt-spray environment. *Construction and Building Materials, 316*, 125878. doi: 10.1016/j.conbuildmat.2021.125878
12. Dou X., Yu H., Ma H., Da B., Yuan Y., Mi R., Zhu H. (2016): Surface chloride concentration profiles of coral concrete exposed to marine environment. *Bulletin of the Chinese Ceramic Society, 35*(9), 2695-2700.
13. Sun D., Cao Z., Wu K., Schutter G., Zhang L. (2022): Degradation of concrete in marine environment under coupled chloride and sulfate attack: A numerical and experimental study. *Case Studies in Construction Materials, 17*, e01218. doi: 10.1016/j.cscm.2022.e01218
14. Chang H., Jin Z., Zhao T., Wang B., Li Z., Liu J. (2020): Capillary suction induced water absorption and chloride transport in non-saturated concrete: The influence of humidity, mineral admixtures and sulfate ions. *Construction and Building Materials, 236*, 117581. doi: 10.1016/j.conbuildmat.2019.117581
15. Chen X., Tang M., Ma K. (2012) Underground concrete structure exposure to sulfate and chloride invading environment. *Journal of Central South University, 43*(7), 2803-2812.
16. Jin Z., Sun W., Zhang Y., Jiang J., Liu J. (2007): Interaction between sulfate and chloride solution attack of concretes with and without fly ash. *Cement and Concrete Research, 37*,1223–1232. doi: 10.1016/j.cemconres.2007.02.016
17. Du J., Jiao R., Ji Y. (2012): The reduction in sulfate corrosion of concrete by chloride ion. *Zhongguo Kuangye Daxue Xuebao(Journal of China University of Mining & Technology), 41*(6), 906-911.
18. Li D., Li L., Wang Y. (2022) Modelling of convection, diffusion and binding of chlorides in concrete during wetting-drying cycles. *Marine Structures, 84*, 103240. doi: 10.1016/j.marstruc.2022.103240
19. Cheng S., Wu Z.., Wu Q., Chen X., Shui Z., Lu J. (2022): Degradation characteristics of Portland cement mortar incorporating supplementary cementitious materials under multi-ions attacks and drying-wetting cycles. *Journal of Cleaner Production, 363*, 132378. doi: 10.1016/j.jclepro.2022.132378
20. Sun D., Huang C., Cao Z., Wu K. (2021): Reliability assessment of concrete under external sulfate attack. *Case Studies in Construction Materials, 17*, e00690. doi: 10.1016/j.cscm.2021.e00690
21. Yin Y., Hu S., Lian J., Liu R. (2022): Fracture properties of concrete exposed to different sulfate solutions under drying-wetting cycles. *Engineering Fracture Mechanics, 266*, 108406. doi: 10.1016/j.engfracmech.2022.108406
22. Zhao K., Qiao Y., Zhang P., Bao J., Tian Y. (2020): Experimental and numerical study on chloride transport in cement mortar during drying process. *Construction and Building Materials, 258*, 119655. doi: 10.1016/j.conbuildmat.2020.119655
23. Praseeda D., Rao K. (2022): Investigation of sulphate resistance of the nano reinforced blended concrete. *Cleaner Materials, 3*, 100047. doi: 10.1016/j.clema.2022.100047
24. Liu P., Chen Y., Wang W., Yu Z. (2020) Effect of physical and chemical sulfate attack on performance degradation of concrete under different conditions. *Chemical Physics Letters, 745*, 137254. doi: 10.1016/j.cplett.2020.137254
25. Song L., Sun W., Gao J. (2012): Influence of curing age on time dependence of chloride diffusion coefficient of concrete. *Journal of Southeast University, 43*(7), 2803-2812.
26. Wang Y., Liu Z, Fu K., Li Q., Wang Y. (2020): Experimental studies on the chloride ion permeability of concrete considering the effect of freeze–thaw damage. *Construction and Building Materials, 236*, 117556. doi: 10.1016/j.conbuildmat.2019.117556
27. Zhang B., Zhang Y., Shi J., Liu T., Zhuang H. (2016): Long-term variability of chloride diffusion coefficients of concrete under the strong tidal environment. *Concrete, 6*, 35-37.
28. Ou F., Zhang J., Liu G., Zhao S. (2022): Experimental study on chloride ion diffusion in concrete affected by exposure conditions. *Materials, 15*, 2917-2928. doi: 10.3390/ma15082917
29. Cheng S., Shui Z., Sun T., Yu R., Zhang G., Ding S. (2017): Effect of fly ash, blast furnace, slag and metakaolin on mechanical properties and durability of coral sand concrete. *Applied Clay Science, 141*, 111-117. doi: 10.1016/j.clay.2017.02.026
30. Gao R., Li Q., Zhao S. (2013): Concrete deterioration mechanisms under combined sulfate attack and flexural loading. *Journal of Materials in Civil Engineering, 25* (1), 39-44.
31. Jiang L. (2014): Study on deterioration of concrete under sulfate attack. PhD Dissertation, Xi'an University of Architecture and Technology.